Journal of Theoretical and Applied Mechanics, Sofia, Vol.52 (2022) pp. 277-293
INTERDISCIPLINARY TOPICS

DESIGN AND PERFORMANCE OF DEMONSTRATOR OF AUTONOMOUS FIXED WING UAV CATLTR

VALENTIN PENEV*

Institute of Mechanics, Autonomous Platforms,
Bulgarian Academy of Sciences, Acad. G. Bonchev Str., Bl. 4, Sofia, Bulgaria

[Received: 14 October 2021. Accepted: 05 April 2022]

doi: https://doi.org/10.55787/jtams.22.52.3.277

ABSTRACT: The demonstrator of fixed wing UAV is designed for visual detection, recognition, segmentation and tracking of cattle from the air. It will help veterinarian doctors with remote determination of physiology state. Some of challenges of visually tracking autonomous flying platform, that accurate trajectory control has had so far, have been in certain instances avoidable. Full simulator in SIMULINK was developed for a vehicle dynamics, sensors and its guidance algorithms. Advanced approach for determination of platform attitude is used to enhance accuracy of guidance. Novel model-based control and its algorithm for tuning are proposed and tested in the simulation and real flight. Partial flight log data is compared to that of the proposed model and it is shown that the model accurately replicates the true flight dynamics. The strapped-down seeker model passes the deflections of the target from Line-of-Sight to the autopilot. The results predict that the vehicle's performance in response to excessive roll, pitch and yaw is extremely sensitive to the quality of guidance. The joint simulation model demonstrated was highly dependent on failure of the seeker used for guidance due to oscillation at some degree of the roll, pitch and yawing of the airframe.

KEY WORDS: fixed wing UAV, AHRS, complementary filter, model-based control, visual tracking, flight simulation, and tandem aircraft.

1 INTRODUCTION

CATLTR system is primarily designed to detect segment and track the cattle (further the target will be used instead of cattle). The CATLTR is a small size fixed wing platform, which is hand held launched. The introduction of system equipped with two cameras daylight and infrared into the modern husbandry has given veterinarians the ability remotely find a physiology state of cattle. The operating range is about 15 km and flight time is about an hour. Once the target field is identified into the map,

*Corresponding author e-mail: v.penev@imbm.bas.bg

the vehicle will fly autonomously to the field and will start loitering to identify the cattle - target. The vehicle needs further operator input during flight to lock individual object. By its nature, CATLTR system should use precision sensors (tactical grade) and guidance, but it was decided to use low-cost sensors and try to achieve best performance from them. It was one of the goals of the research to investigate low-cost attitude reference heading system to meet the requirement for high precision guidance.

The work reported here develops a six degree-of-freedom (DOF) model [1–4]] of the CATLTR vehicle. In addition, a guidance algorithm is developed to mimic the flying modes of the actual system. The aerodynamics of the airframe and control surfaces are modeled separately to isolate possible changes from interaction and demonstrate their effects in simulation. Partial test flights of a CATLTR are used to verify the accuracy of the proposed model and guidance algorithms. The CATLTR is roll controlled and it is also demonstrated that the orientation of the strapped-down seeker around the airframe is a significant factor in its response to damage.

2 BACKGROUND

The system is a two-parts tool consisting of a ground control unit (GCS) and a CATLTR vehicle. The CATLTR vehicle is a handheld launched. The CATLTR vehicle airframe shown in Fig. 1 consists of a 2 inches diameter body, two mid-body wings and rudder. The control surfaces are chosen to be ailerons, elevators, flaps and rudder. The set of control surfaces could be reduced to elevons only without loss of controllability and precision. Elevons or tailerons are aircraft control surfaces that combine the functions of the elevator and the aileron.

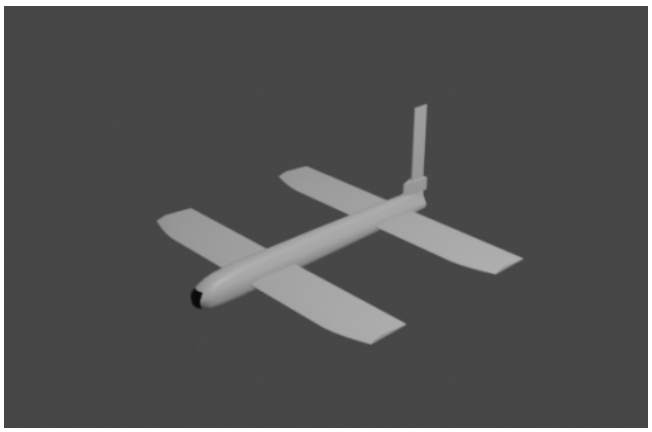

Fig. 1: The geometry of CATLR.

Attitude Heading Reference System (AHRS) calculates the orientation of the vehicle. The visual tracking system (VTS) or strapped-down seeker module consists of two cameras daylight and IR. Both cameras have their own processor who process the video stream and feed the autopilot with coordinates of displacement of target to LoS and additional information. The two processors are responsible for detection and segmentations of the target and on this stage; they exchange the information about the detected "blobs". Flight Control System (FLCS) generates control surface commands. The GCS shows video streams from both on-board cameras is a control unit used by the operator to lock the target or manually detect and identify targets. Guidance is based on infrared and daylight seekers requiring the target to remain in the squared area of interest around the line of sight (LOS). Moreover, to a LOS view the seeker must have limited roll with respect to the target to maintain a lock with the target. The first problem occurs when the seeker maintains view of the target but the guidance responds poorly to moving target. The second type of failure occurs when excessive yaw, pitch or roll causes seeker failure. The third problem is the accuracy of attitude determination and it is of primary importance. Of course, the requirement for low cost AHRS plays significant role. This research uses simulation to predict the response of a CATLTR to both types of trajectories midcourse and terminal stage and estimate the probability of failure in both cases. The second phase of flight is climb out. The CATLTR climbs at a constant rate until one of two constraints met, the CATLTR reaches an altitude of 100 m, or the line of sight (LOS) of the seeker nears its maximum value. The flight of autonomous platform [5] has four stages: Launch; Climb; Loitering (midcourse); Terminal.

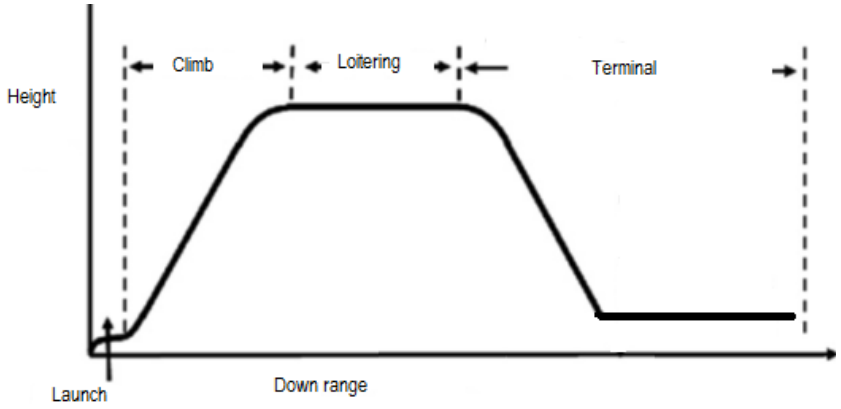

Fig. 2: Flight stages of platform.

3 Flight Dynamics Modeling and Simulation of Fixed Wing UAV

According to mission requirements, previous experience and analysis of contemporary achievements the tandem fixed wing configuration was selected (Fig. 1. Tandem aerodynamic configuration has fewer oscillations in roll, pitch and azimuth and good controllability.

3.1 Defining vehicle geometry

The geometry of this tandem fixed-wing platform is described below. The original design objective for this geometry was a general aviation UAV that was safe, simple to fly, and easily maintainable with specific mission and performance constraints. Potential performance requirements for this aircraft include: level cruise speed; acceptable rate of descent and climb; acceptable stall speed; controllable low-level velocity flight. The partial input set for calculating the forces, moments, aerodynamic coefficients and derivatives is given in Table 1.

Table 1: CATLTR UAV geometry

CATLTR UAV Specifications			
Wingspan	0.6 m	Fuselage length	0.725 m
Max speed	170 km/h	Cruise speed	40 km/h
Max altitude	300 m	Max takeoff weight	5 kg
Flight path angle during terminl stage	-1 to 3°		

3.2 Determining vehicle aerodynamic characteristics

The aircraft's geometrical configuration determines its aerodynamic characteristics, and therefore its performance and handling qualities.

"Tornado" Vortex Lattice Method [6] was used to define the fixed wing UAV set of aerodynamics parameters. Analytical prediction is a quicker and less expensive way to estimate aerodynamic characteristics in the early stages of design. The airframe model incorporates several key assumptions and limitations: The airframe is rigid body and has constant mass, center of gravity, and inertia; CATLETR is laterally symmetric vehicle; Control effectiveness varies nonlinearly with angle of attack and linearly with angle of deflection and air velocity. Control effectiveness is not dependent on sideslip angle. One major assumption made to implement Tornado's vortex lattice theory is the presence of small angles of attack. So, Tornado cannot be trusted to provide useful results with large angles of attacks or large rotational speeds.

3.3 AERODYNAMIC COEFFICIENTS FOR CONSTRUCTING FORCES AND MOMENTS

Tandem aircraft is a typical fixed-wing UAV with geometry and control surfaces [1, 3, 7, 8]. The typical airframe model consists of a number of subsystems, such as: equations of motion; environmental models; calculation of aerodynamic coefficients, forces, and moments; environmental models; alpha, beta, mach ; aerodynamic coefficients ; forces and moments. All look-up tables calculated by Tornado [6] are implemented in the flight model – CX, CY, CZ, Cl, Cm, Cn, CX_d, CY_d, CZ_d, Cl_d, Cm_d, Cn_d, CX_P, CY_P, CZ_P, Cl_P, Cm_P, Cn_P, CX_Q, CY_Q, CZ_Q, Cl_Q, Cm_Q, Cn_Q, CX_R, CY_R, CZ_R, Cl_R, Cm_R, Cn_R, C_{lift}, C_{drag}. Body-fixed reference frame is used, to specify forces, moments and angles.

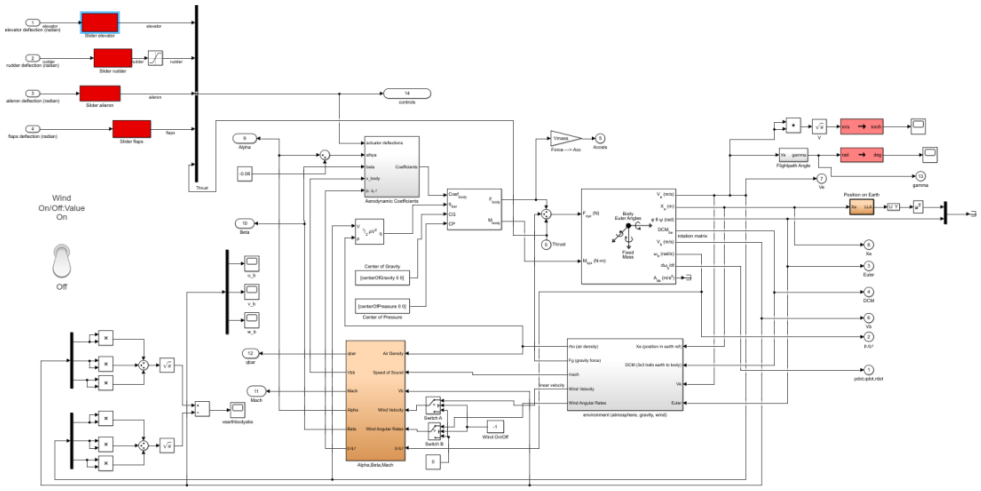

Fig. 3: SIMULINK model of flight dynamics.

The result of calculation of aerodynamic coefficients split in three standard categories: Datum coefficients; Damping coefficients; Control surface deflection coefficients.

4 ATTITUDE HEADING REFERENCE SYSTEM

The precise inertial navigation system (INS) supported by GPS is able to assist VTS with tracking the target in GE mode, where the altitude of the platform is significantly small and as a result the range of tracking is short. The requirements on the strapped AHRS, INS and FLCS are high. AHRS embrace two subsystems: Regular AHRS with accelerometers, velocity gyros, magnetometers, barometer and Pitot tube sensor and Gyro-Free AHRS (GFAHRS) redundant array of accelerometers [9, 10].

The proposed approach will significantly improve the quality of determination of the attitude and position of the platform and will make the tasks of the FLCS and gyro-stabilization of the 3D-gymbal easier (not required in this research). The novel approach, based on gradient descent algorithm and explicit complementary filter [11], computes in a more precise and stable way the attitude, quadratic representation of angular velocity and angular and linear accelerations. The extended Kalman filter and GFAHRS [10] with nine accelerometers are used as redundant. However, accelerations generated by the vehicle in the dynamic mode strongly affect the accelerometer measurements. The relationship is expressed using the rigid body motion equation [8, 9] as:

$$\begin{bmatrix} a_x \\ a_y \\ a_z \end{bmatrix} = \begin{bmatrix} g_x \\ g_y \\ g_z \end{bmatrix} - \begin{bmatrix} \dot{v}_x + \omega_y v_z - \omega_z v_y \\ \dot{v}_y + \omega_z v_x - \omega_x v_z \\ \dot{v}_z + \omega_x v_y - \omega_y v_x \end{bmatrix}, \tag{1}$$

$$\begin{bmatrix} g_x \\ g_y \\ g_z \end{bmatrix} \cong \begin{bmatrix} \dot{v}_x + a_x \\ a_y + \omega_z v_x \\ a_z - \omega_y v_x \end{bmatrix}. \tag{2}$$

Equations (1) and (2) describes the simplified way for separation gravity force vector components g_x, g_y and g_z from measurements a_x, a_y and a_z, where $\dot{v}_x$, $\dot{v}_y$ and $\dot{v}_z$ are accelerations developed by platform.

This research introduces useful variation to orientation filter [11, 12] that is applicable to both IMUs and MARG sensor arrays addressing issues of computational load and parameter tuning associated with Kalman-based approaches. A complete derivation and empirical evaluation of the new filter is presented. Rotational matrix ${}^{A}_{B}R$ of compounded orientation ${}^{S}_{E}\hat{q}$ in current complementary filters is defined as:

$${}^{A}_{B}R = \begin{bmatrix} 2q_1^2 - 1 + 2q_2^2 & 2(q_2q_3 + q_1q_4) & 2(q_2q_4 - q_1q_3) \\ 2(q_2q_3 - q_1q_4) & 2q_1^2 - 1 + 2q_3^2 & 2(q_3q_4 + q_1q_2) \\ 2(q_2q_4 + q_1q_3) & 2(q_3q_4 - q_1q_2) & 2q_1^2 - 1 + 2q_4^2 \end{bmatrix}.$$

Many optimization algorithms exist but the gradient descent algorithm is one of the simplest to both implement and compute. Equation (3) describes the gradient descent algorithm in an orientation estimation of ${}^{S}_{E}\hat{q}_{n+1}$ based on an 'initial guess' orientation ${}^{S}_{E}\hat{q}_0$ and a step-size μ. Equation (4) computes the gradient of the solution surface defined by the objective function and its Jacobian; simplified to the 3 row vectors defined by equations (5) of objective function respectively.

$${}^{S}_{E}\hat{q}_{k+1} = {}^{S}_{E}\hat{q}_k - \mu \frac{\nabla f({}^{S}_{E}\hat{q}_k, E\hat{d}, s\hat{s})}{\left\| \nabla f({}^{S}_{E}\hat{q}_k, E\hat{d}, s\hat{s}) \right\|} \quad k = 0, 1, 2 \ldots, n, \tag{3}$$

$$\nabla f\left({}^{S}_{E}\hat{q}_k, E\hat{d}, s\hat{s}\right) = J^t\left({}^{S}_{E}\hat{q}_k, E\hat{d}\right) f\left({}^{S}_{E}\hat{q}_k, E\hat{d}, s\hat{s}\right), \tag{4}$$

$$f\left({}^{S}_{E}\hat{q}_k, E\hat{d}, s\hat{s}\right) = \tag{5}$$

$$= \begin{bmatrix} 2d_x\left(\frac{1}{2} - q_3^2 - q_4^2\right) + 2d_y(q_1q_4 + q_2q_3) + 2d_z(q_2q_4 - q_1q_3) - a_x \\ 2d_x(q_2q_3 - q_1q_4) + 2d_y\left(\frac{1}{2} - q_2^2 - q_4^2\right) + 2d_z(q_1q_2 + q_3q_4) - a_y \\ 2d_x(q_1q_3 + q_2q_4) + 2d_y(q_3q_4 - q_1q_2) + 2d_z\left(\frac{1}{2} - q_2^2 - q_3^2\right) - a_z \end{bmatrix}.$$

Equations (3) to (4) describe the general form of the algorithm applicable to a field predefined in any direction. However, an appropriate convention would be to assume that the direction of gravity defines the y and z-axes only. The assumption originated from simulations, some test flights (acceleration records) and trajectory of the flight. Then simplified Jacobian is in equation (6)

$$f\left({}^{S}_{E}\hat{q}_k, E\hat{d}, s\hat{s}\right) = \begin{bmatrix} 2(q_1q_4 + q_2q_3) + 2(q_2q_4 - q_1q_3) - a_x \\ 2\left(\frac{1}{2} - q_2^2 - q_4^2\right) + 2(q_1q_2 + q_3q_4) - a_y \\ 2(q_3q_4 - q_1q_2) + 2\left(\frac{1}{2} - q_2^2 - q_3^2\right) - a_z \end{bmatrix}$$

$$J\left({}^{S}_{E}\hat{q}_k, E\hat{d}\right) = \begin{bmatrix} 2q_4 - 2q_3 & 2q_3 + 2q_4 & 2q_2 - 2q_1 & 2q_1 - 2q_2 \\ 2q_2 & 2q_1 - 4q_2 & 2q_4 & 2q_3 - 4q_4 \\ -2q_2 & -4q_2 - 2q_1 & 4q_3 + 2q_4 & 2q_3 \end{bmatrix}. \tag{6}$$

A priory the readings from velocity gyros and accelerometers have been filtered. Accelerometer readings have been subtracted by estimated linear $\dot{v}_y$ and $\dot{v}_z$, which are calculated by equations of aerodynamic force and moment coefficients used in flight dynamics simulation model [6, 13].

$$C_{X_a} = C_{X_0} + C_{X_\alpha}\alpha + C_{X_{\alpha^2}}\alpha^2 + C_{X_{\alpha^3}}\alpha^3 + C_{X_q}\frac{q\bar{c}}{V} + C_{X_{\delta_r}}\delta_r + C_{X_{\delta_f}}\delta_f + C_{X_{\alpha\delta_f}}\alpha\delta_f,$$

$$C^*_{Y_a} = C_{Y_0} + C_{Y_\beta}\beta + C_{Y_p}\frac{pb}{2V} + C_{Y_r}\frac{rb}{2V} + C_{Y_{\delta_\alpha}}\delta_\alpha + C_{Y_{\delta_r}}\delta_r + C_{Y_{\delta_r\alpha}}\delta_r\alpha,$$

$$C_{Z_a} = C_{Z_0} + C_{Z_\alpha}\alpha + C_{Z_{\alpha^3}}\alpha^3 + C_{Z_q}\frac{q\bar{c}}{V} + C_{Z_{\delta_e}}\delta_e + C_{Z_{\delta_e\beta^2}}\delta_e\beta^2 + C_{Z_{\delta_f}}\delta_f + C_{Z_{\alpha\delta_f}}\alpha\delta_f,$$

$$C_{l_a} = C_{l_0} + C_{l_\beta}\beta + C_{l_p}\frac{pb}{2V} + C_{l_r}\frac{rb}{2V} + C_{l_{\delta_\alpha}}\delta_\alpha + C_{l_{\delta_r}}\delta_r + C_{l_{\delta_\alpha\alpha}}\delta_\alpha\alpha,$$

$$C_{m_a} = C_{m_0} + C_{m_\alpha}\alpha + C_{m_{\alpha^2}}\alpha^2 + C_{m_q}\frac{q\bar{c}}{V} + C_{m_{\delta_e}}\delta_e + C_{m_{\beta^2}}\beta^2 + C_{m_r}\frac{rb}{2V} + C_{m_{\delta_f}}\delta_f,$$

$$C_{n_a} = C_{n_0} + C_{n_\beta}\beta + C_{n_p}\frac{pb}{2V} + C_{n_r}\frac{rb}{2V} + C_{n_{\delta_\alpha}}\delta_\alpha + C_{n_{\delta_r}}\delta_r + C_{n_q}\frac{q\bar{c}}{V} + C_{n_{\beta^3}}\beta^3.$$

In addition, noisy sensor measurements should be pre-filtered before introducing them into the system, especially if the noise is electronic or high frequency vibra-

tional disturbances above the bandwidth of the vehicle performance. Furthermore, sensor misalignment, temperature drift, and center of gravity (CG) offsets should be included based on calibration data [5, 9, 11]. Furthermore, with high- speed maneuvers, the Kalman filter is usually utilized to fuse the multiple sensor data.

5 VISUAL TRACKING SYSTEM

VTS will be able to detect and recognize the targets. Object detection and tracking are two of the most important topics in computer vision. Object detection is the process of automatically detecting objects of importance with respect to some criterion in an image. The real-time and robust procedure is used for visual tracking of an object not included in the target repository of known targets. The VST will give an additional extra feature to create a pattern recognition library of visual images for an object during the flight and on the ground. The lock will be either manual or automatic. As it was mentioned above, the manual Lock will allow reliable tracking of any object.

A flying platform equipped with VTS will be able to operate in the following way with the locked target: Follow the target at appropriate distance; Visual homing based on model-based control and proportional navigation and guidance algorithm to cow; Loitering relative to a cow or target

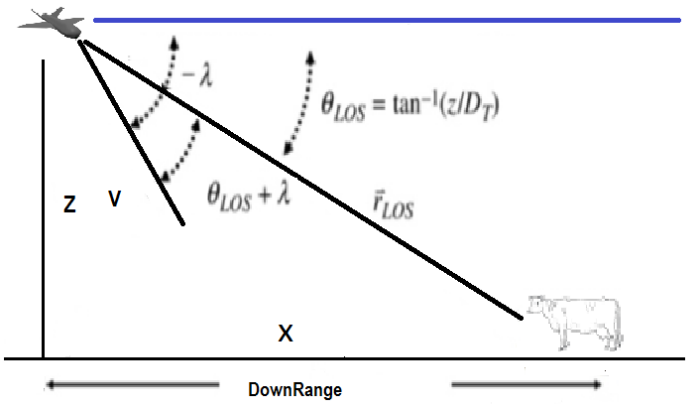

Fig. 4: 2-D geometry of LoS.

Angular velocity of LoS is given in the next equation.

$$\omega_{\text{LOS}} = \frac{V}{|\vec{r}_{\text{LOS}}|} sin\left(\theta_{\text{LOS}} + \lambda = \text{FPA}\right).$$

There are many issues when object detection and tracking are performed on images captured from a UAV. The UAV moves with relatively high velocity. Since a limited

amount of images captured each second, the velocity and altitude determines how much consecutive images change. Larger altitude leads to less change. Unfortunately, larger altitudes also cause each object in the image to be smaller and harder to detect. For tracking purposes, it is beneficial to have the object of interest inside the Field of View (FoV) of the camera during the tracking period. A UAV moving with large velocity will capture images where the object of interest is visible for a limited amount of image frames only. Only moving objects are of interest. Slowly moving objects and motion of target caused by the motion of the platform might be hard to detect, since the static parts of the image will change almost equally much as the object.

Adaptive background model, which continuously updates the background model, works well for the fixed-wing UAV velocity. Tracking the target is performed only in particular rectangular area of interest (AoI) – left upper and right bottom red corners in Fig. 5. The adaptive LoS is used as well as, which means position of LoS and size of AoI are moving across the frame buffer. Mean shift segmentation is a famous segmentation algorithm. The region matching method used here is a template matching approach based on normalized cross-correlation. The displacements of nine templates [14], created symmetrically across the images, are used to find nine OF vectors. Template matches below a given threshold are discarded and the corresponding OF vector removed. Unreliable matches generated by VTS can occur in case of uniform terrain, changes in brightness or simply when the area covered by the template has disappeared from the image in the time between the captured frames.

A natural approach to detect grey level blobs [14] is to associate a bright (dark) blob with each local maximum else, it has one or more higher neighbors, which are all

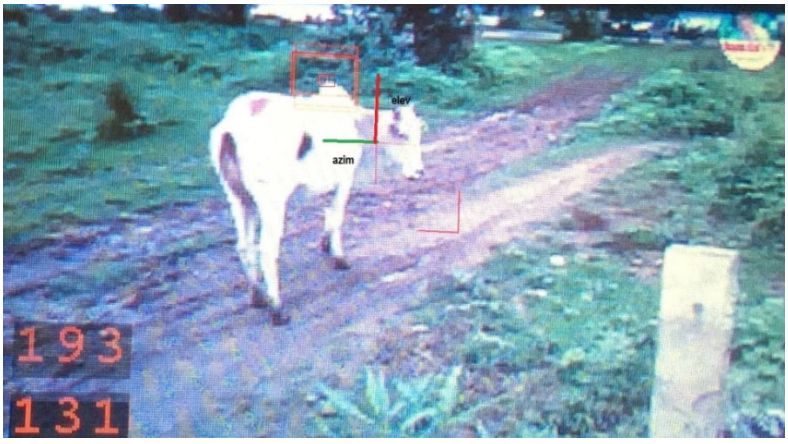

Fig. 5: Screenshot from real-time tracking device.

parts of the same blob. One approach to identifying a pattern within an image uses cross correlation of the image with a suitable mask. Haar-like feature descriptors were successfully used to implement the real-time cow detector. The VTS is based on two algorithms, a descriptor of the image type Haar-like, a cross-correlation algorithm, adaptive background and adaptive LoS. That combination provides robustness in tracking the cow against all negative influences: oscillations in roll, pitch and yaw; multiple moving objects; significant changes in background; variation of the target distance in tracking process. The resolution of daylight camera is at least 640×480, but only the grayscale pixels of AoI are transferred to embedded processor memory. The same approach is used with infrared imagery. The embedded processors power allows having a 15-20 frames per second.

6 Model Based Control

Successful real-time implementation of trajectory guidance algorithms has employed approximate methods, that either assume some knowledge of the flight mechanics and/or make assumptions to reduce the dimensionality of the dynamical system. Instead, intuitive and robust MB control is used. The advantages of proposed algorithm are: no needs for extended computational power; off-line procedure for tuning the parameters of control; robust control to the changes of flight parameters and environment; this implementation eliminates the need for guidance to generate the angle-of-attack command; no needs for relatively big angles of attack – average is 3-4°; the roll or pitch commands are determined based on a relative position of vehicles. The control law was the key part of the guidance system, which had important effect to the guidance performance [13]. The model based control law could reduce the miss distance due to target maneuvering and the guidance system dynamics [13,15]. In order to use optimal guidance law, the guidance information should be estimated above all. For the vehicle with estimated guidance signal, the acceleration command would be noisy. That demanded the autopilot should be robust as well as reliabile. Many different forms of autopilot had been studied in some literatures [5–8, 13, 15].

6.1 2-Loops model based control

The reference model has two feedback signals proportional and velocity, shown in the next figure. The ranges of feedback gains are defined in the following way:

$$K_{\text{pr}} = (PR_{\min}, PR_{\max}); \quad K_{\text{vr}} = (VR_{\min}, VR_{\max}) .$$

Position and velocity reference models are defined as:

$$F_{\text{posRM}} = \frac{g}{ts + a} ; \qquad F_{\text{velRM}} = \frac{gs}{ts + a} .$$

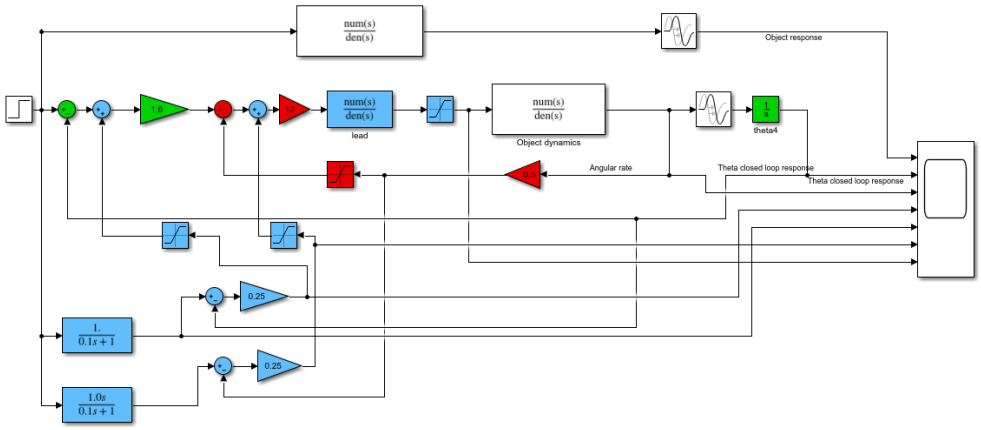

Fig. 6: 2-Loops MB control with simplified object dynamics.

Proposed scheme is two loops control law, where the position is calculated first. Another interesting point is reference model of velocity shown in Fig. 6 that velocity reference model is differentiated position reference model. Instead, another velocity reference model was successfully used and that model could be the one who meets specific requirement.

$$F_{\text{velRM}} = \frac{(g+G)s}{(t+T)s+(a+A)} \ ,$$

where g, t and a are normal parameters from position reference model transfer function. That difference G, T and A could be included in searching procedure.

6.2 3-Loops model based control

Vehicle with estimated guidance signal has noisy acceleration command. That needs the robust and reliability FLCS. Many different forms of autopilot had been studied. Three-loop MB control in Fig. 7 with pseudo-angle of attack feedback had good robustness, which could be used to make sure the flight vehicle operates well.

The ranges of feedback gains are defined in the following way:

$$K_{\text{pr}} = (PR_{\min}, PR_{\max}); \quad K_{\text{vr}} = (VR_{\min}, VR_{\max}); \quad K_{\text{ar}} = (AR_{\min}, AR_{\max})$$

and for each range is defined a step d_{pp}, d_{vp} and d_{ap}. Three nested loops which move the current values of the gains with appropriate step determines the simple algorithm doing full scale search through the ranges. During the run-time parameters of each transition-time process or frequency domain characteristics are stored and the best solution according to proper criteria is chosen. There are several saturations

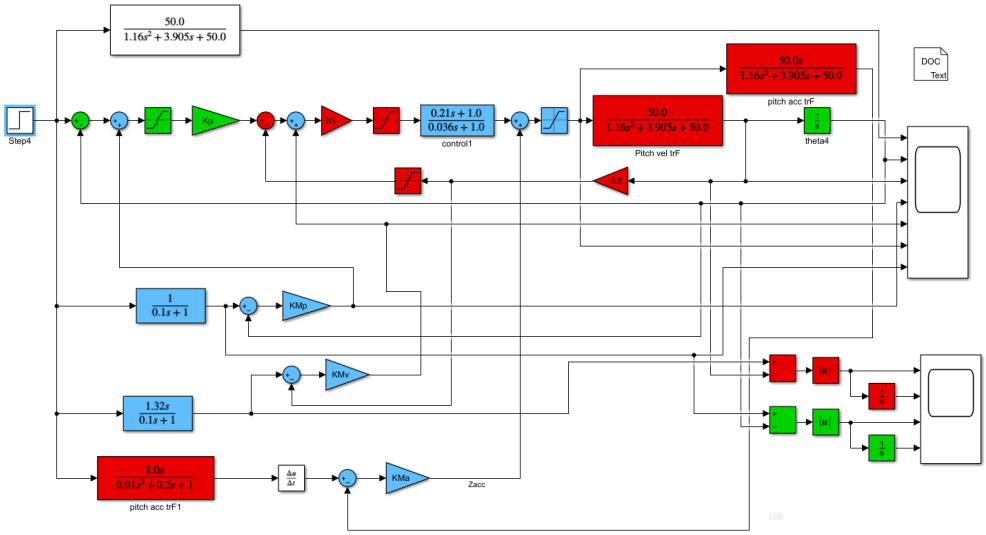

Fig. 7: 3-Loops MB control with simplified object dynamics.

in the position, velocity and accelerations loops, they are defined in the same way and added to search algorithm. The same approach is used either transfer function which describe the roll or pitch dynamics or complete 6DoF flight dynamics model. The algorithm was implemented in Matlab.m, which opens the SIMULINK model and start the three nested loops for each step change. The parameters of time domain and frequency domain responses are stored and evaluated for best solution. That is a numerical solution for complex problem of analytical tuning of gains of model-based control. It avoids stopping at local extrema. The time required for calculations depends on complexity of flight dynamics models.

6.3 Adaptive Model Based Control

For real systems, we can add loops with air velocity and AoA. In this case, the gain will be a look-up table with the inputs of AoA and air velocity. The selection criteria and parameters of transition process are multifaceted. For that reason, velocity control block and AoA setup block are added to simulation solution with 6DoF, see Fig. 8. During the tuning procedure that block could easily change the current AoA.

Diagram of adaptive model based control is illustrated in Fig. 9.

MBC has some advantages to standard Proportional-Integral-Derivative control in terms of performance and MBC method outperforms a gain-scheduled PID controller in all performance areas such as overshoot, worst-case settling time, and robustness against system variations, at the expense of a slight increase in sensitivity to sensor

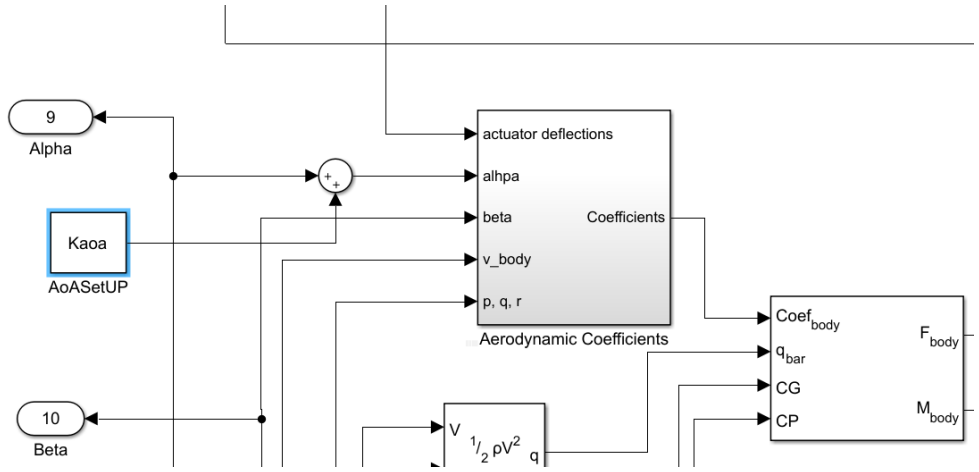

Fig. 8: Additional AoA Setup block, which allows adding angle of attack to search algorithm.

noise. The MBC provides similar behaviors as those found with the more complex algorithms lake LQG, but has the benefits of a simplified and more intuitive scheme, even when the saturation parameters are added to dynamic parameters of position, velocity and acceleration references systems. The AHRS and FLCS were built on ESP32 and some performance tests are listed in Table 2.

Table 2: Performance of AHRS/FLCS processor

Four complementary AHRS algorithms (acc, rate gyro, magnetometers, altimeter)	Total time 62 micro sec. One of the algorithms is stable above 12 G
Flight dynamics model (mid level of accuracy, 32 look-up tables) appropriate for inverse dynamics control and predictor	2 ms
Model based control with reference model (position, velocity and acceleration), and removing the Gravity (steep turns)	2.3 ms

Of course, that extends the time for finding complete solution, but avoids the case where you find a local extremum. The process of tuning of a MBC reduces to adjusting a simple reference 'bandwidth' in order to achieve the desired performance for the specific vehicle. The design of the controller has two key elements: finding performance-relevant reference system dynamics; tuning the parameters of controller.

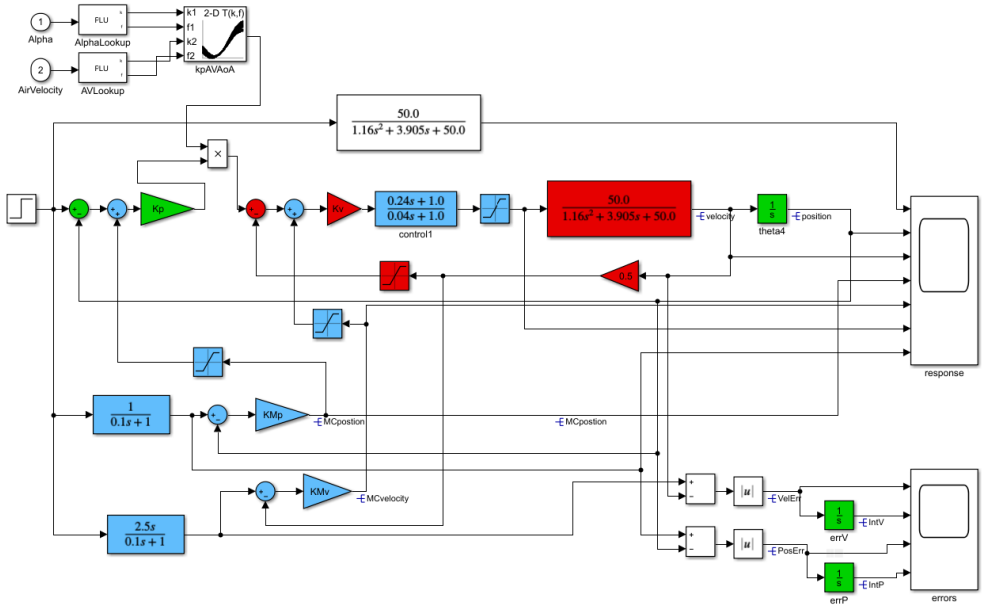

Fig. 9: Adaptive model-based control.

Once a control-relevant model is derived, tuning of the MBC is quite straightforward. Input to the model based control could be either the azimuth and elevation distances or their derivatives, which are somewhat angular velocities of LOS.

7 Creating Flight Vehicle Simulation

The core element of the Simulink model is a nonlinear version of the rigid body dynamics of the UAV platform [4]. The aerodynamic forces and moments acting on CATLTR UAV are generated from coefficients that are non-linear functions of roll, pitch and air velocity. The main elements of joint simulations Fig. 11 are listed below: flight dynamics + MBC showed in Fig. 10; visual tacking system; target motion model; seekers model.

An extended functionality attitude dynamics, sensors and control simulator (depicted in Fig. 11) was developed to facilitate research into improving techniques for the attitude control of tandem fixed wing aircraft. The proposed AHRS is a part of the block '3-loops MBC-FLCS'. The simulation of visual tracking system has two separate subsystems. The first one gets LoS azimuth and elevation errors directly from mechanical motion model of the target and it is noiseless. The second one is to use a real video of moving target or artificially generated video from equations of motion of the target.

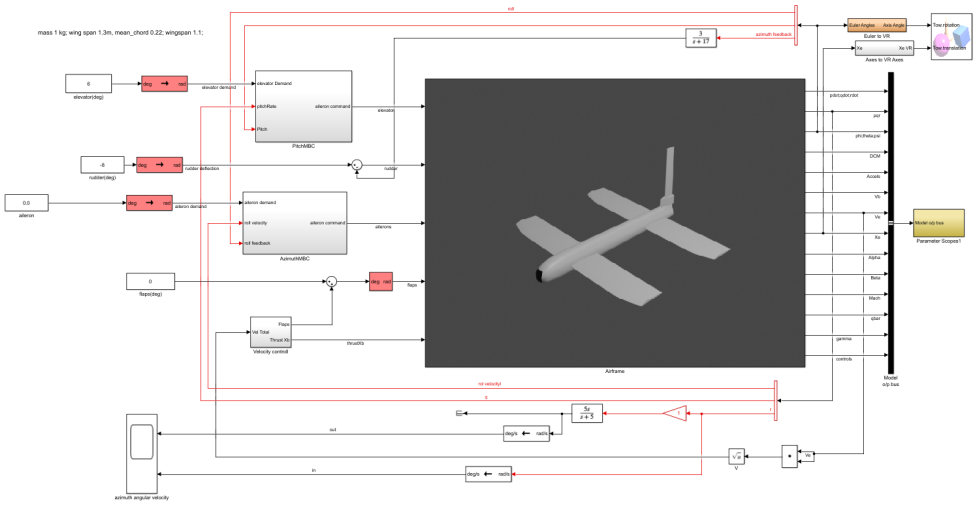

Fig. 10: Flight dynamics and model based control.

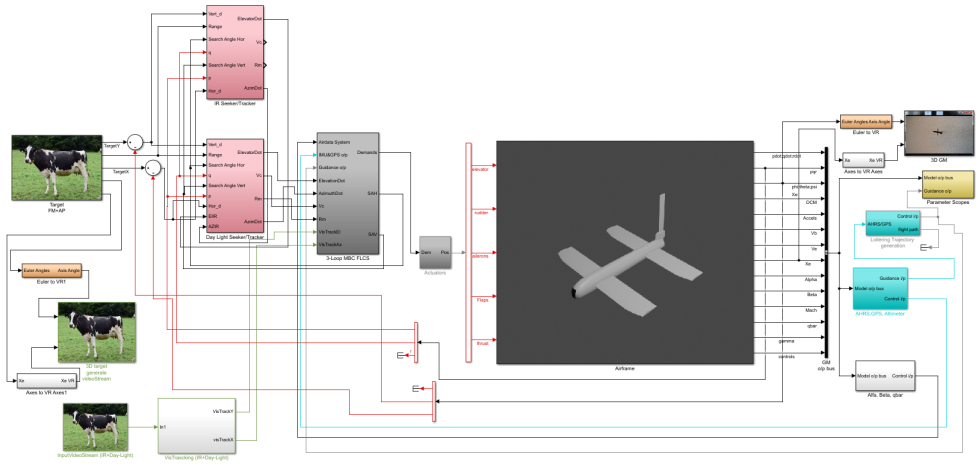

Fig. 11: Joint simulation model – SIMULINK.

If the altitude reaches 30 m without the LOS reaching its threshold, the vehicle transitions to altitude hold. As the vehicle approaches the target in altitude, hold mode the seeker angle becomes increasingly negative. Terminal guidance puts the CATLTR on a trajectory for target interception by maintaining a constant seeker angle. Guidance during all stages uses three error signals: roll error, pitch error, and yaw error as well as their derivatives.

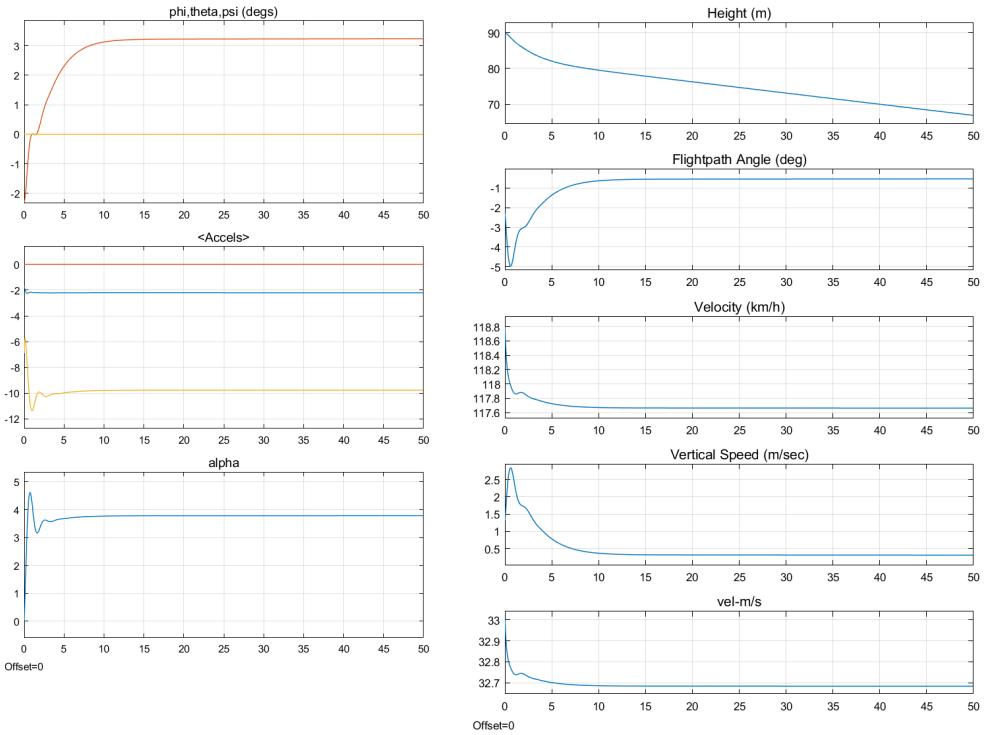

Fig. 12: Some of flight parameters during the simulation (mass is 8 kg).

The nonlinearity in transition process of flight path angle is because of velocity reference model is not first derivative of position reference model. In spite, nonlinear 6 DoF the transition process of roll pitch and yaw are very close to the first-order reference model. The oscillation in pitch with amplitude exceeding 3° causes loss of target by VTS.

8 Conclusion

The proposed three-loop autopilot with pseudo-angle of attack feedback has strong robustness. From the simulation, it could be shown that after a short transient time, the estimated guidance signal could converge to their real values. The command acceleration obtained from optimal guidance law was noisy at the transient time, after the transient time it was much smooth and finally concentrated to nearly zero at the end. Three-loop autopilot worked well, which filtered the noise and tracked the command angles, angular velocities and accelerations well. The proposed guidance and control method could reach the request of the flight vehicle with strap-down seeker.

ACKNOWLEDGEMENT

The research leading to these results has received funding from the Ministry of education and science under the National science program INTELLIGENT ANIMAL HUSBANDRY, grant agreement No 01-62/18.03.2021.

REFERENCES

[1] D.A. CAUGHEY (2011) "Introduction to Aircraft Stability and Control, Course Notes for Mechanical & Aerospace Engineering". Cornell University, New York, USA, 2011.

[2] E.B. JACKSON, C.L. CRUZ (1992) "Preliminary Subsonic Aerodynamic Model for Simulation Studies of the HL-20 Lifting Body". NASA TM4302 (August 1992).

[3] O. KARAS (2012) "UAV Simulation Environment for Autonomous Flight Control Algorithms". West Virginia University.

[4] V. PENEV (2008) Flight Simulation Kernel. Internal report. Sofia.

[5] O. ARIFIANTO, M. FARHOOD (2015) Development and Modeling of a Low-Cost Unmanned Aerial Vehicle Research Platform. *Journal of Intelligent & Robotic Systems* **80** 139-164.

[6] M. TOMAS (2000) Tornado, a vortex lattice MATLAB implementation for Linear Aerodynamic Wing applications. Master thesis, Royal Institute of Technology (KTH), Sweden, December 2000.

[7] J. ALI, S.A. SALMAN, A.G. SREENATHA, J.Y. CHOI (2006) Attitude Dynamics Identification of Unmanned Aircraft Vehicle. *International Journal of Control, Automation, and Systems* no. 1, 782-787.

[8] V. PENEV, G. ROWLANDS, G. GEORGIEV (2016) Low-Cost Robust High-Performance Remotely Piloted Autonomous Fixed-Wing System. *IJUSEng* **4**(1) 23-36.

[9] V. PENEV (2011) Flight Control System FLCS2.1. Internal report. Sofia.

[10] V.N. PENEV, G.R. ROWLANDS, G.L. GEORGIEV (2017) Novel Approach for Multi-Layered And Redundant AHRS in Spin Stabilized Munition. In: 13th National Congress on Theoretical and Applied Mechanics Sofia, Bulgaria, 6-10th September 2017.

[11] SEBASTIAN O.H. MADGWICK (2010) "An efficient orientation filter for inertial and inertial/magnetic sensor arrays". Report x-io and University of Bristol (UK).

[12] M. EUSTON, P. COOTE, R. MAHONY, J. KIM, T. HAMEL (2007) A complementary filter for attitude estimation of a fixed-wing UAV with a low-cost IMU. In: 6^{th} International Conference on Field and Service Robotics.

[13] R.F. STENGEL (2004) "Flight Dynamics". Princeton University Press, Princeton.

[14] H.H. HELGESEN (2015) "Object Detection and Tracking Based on Optical Flow in Unmanned Aerial Vehicles, Master of Science in Cybernetics and Robotics". Norwegian University of Science and Technology.

[15] V. PENEV, P. ZLATEVA, G. ROWLANDS, G. GEORGIEV (2016) Gyro Stabilized Roll and Pitch Gimbal Controller with Sliding Mode. *IJUSEng* **4**(2) 60-77.